Original Article

Supracerebellar infratentorial inverted subchoroidal approach to lateral ventricle lesions: Anatomical study and illustrative case

Irakliy Abramov[1], Xiaochun Zhao[1], Evgenii Belykh[1], Michael T. Lawton[1], David Pitskhelauri[2], Mark C. Preul[1]

[1]Department of Neurosurgery, Barrow Neurological Institute, Phoenix, Arizona, United States, [2]Department of Neuro-oncology, Burdenko Neurosurgery Center, Moscow, Russian Federation.

E-mail: Irakliy Abramov - irakliy.abramov@dignityhealth.org; Xiaochun Zhao - kyle.g0704@gmail.com; Evgenii Belykh - belykhevgenii@gmail.com; Michael T. Lawton - michael.lawton@barrowbrainandspine.com; David Pitskhelauri - davidpneuro@gmail.com; Mark C. Preul - neuropub@barrowneuro.org

*Corresponding author:
Mark C. Preul,
Department of Neurosurgery,
Barrow Neurological Institute,
Phoenix, AZ, United States.

neuropub@barrowneuro.org

ABSTRACT

Background: This study provides an anatomical description of a novel supracerebellar infratentorial inverted subchoroidal (SIIS) approach to the lateral ventricle. An illustrative case is presented in which this approach was used to simultaneously resect two tumors residing in the posterior fossa and lateral ventricle.

Methods: The SIIS approach was performed on five cadaveric heads using microsurgical and endoscopic techniques. Target points were defined in the lateral ventricle, and quantitative analysis was performed to assess limits of exposure within the lateral ventricle. Two coronal reference planes corresponding to the anterior and posterior margins of the lateral ventricle body were defined. Distances from target points to reference planes were measured, and an imaging-based predicting system was provided according to obtained measurements to guide preoperative approach selection.

Results: Mean (standard deviation) distances between the predefined target points indicating the anterior limits and the anterior plane were 9 (7.0) mm, 11 (5.8) mm, and 7 (5.1) mm; posterior limits had distances of 8 (3.0) mm, 17 (9.2) mm, 15 (9.2) mm, and 9 (7.2) mm to the posterior plane. Limiting factors of the choroidal fissure dissection were the venous angle anteriorly and thalamocaudate vein posteriorly. The position of the venous angle had a high negative correlation with the anterior exposure limit ($r = -0.87$, $P < 0.001$; $r = -0.92$, $P < 0.001$).

Conclusion: A step-by-step anatomical description of a new SIIS approach is given, and a quantitative description of the limits of the exposure is provided to evaluate the application of this approach.

Keywords: Lateral ventricle, Multiple brain lesions, Novel surgical approach, Operative technique

INTRODUCTION

Surgical treatment of patients with multiple brain tumors remains challenging, whether such tumors result from dissemination of a primary central nervous system (CNS) tumor or secondary metastasis. Intracranial metastases are encountered 10 times more often than primary CNS tumors[15] and are now a leading cause of death in high-income countries.[8] Hence, management of multiple tumors has become an increasingly important topic.

In some cases, the dissemination of a neoplastic condition can involve multiple intracranial anatomical compartments. Such circumstances make it challenging to achieve a gross total

resection through a single approach and require multiple surgical stages or multiple craniotomies in a single surgical operation.[3,11,23,26,28] Staging or multiple craniotomies are related to prolonged anesthesia time and a longer hospitalization period, which might increase morbidity, when compared with a single-staged operation.[28]

In this anatomical study, we describe a novel supracerebellar infratentorial inverted subchoroidal (SIIS) approach to the lateral ventricle that has been used with success on cases of ventricular obstruction or caused by tumors residing within the lateral ventricles. It allows removal of lesions within the lateral ventricle and in the posterior fossa during a single-stage surgical operation. We also quantitatively assessed this approach to establish a preoperative prediction system that would allow evaluation of the feasibility of the SIIS approach on the basis of identifiable normal anatomical landmarks on magnetic resonance imaging (MRI) and the location of the lesions in an individualized fashion.

MATERIALS AND METHODS

Five adult human cadaveric heads (mean age, 72 years; male sex, 3) with causes of death that were unrelated to intracranial pathology were obtained and examined. The heads were fixed with a customized alcohol-based solution and a colored silicone vascular injection. Each head was fixed using a Mayfield head holder attached to a dissection station. A stepwise dissection of the approach was performed using standard microsurgical instruments and a clinical grade neurosurgical operating microscope at ×6–×40 magnification (Pentero OPMI, Carl Zeiss Meditec, AG, Oberkochen, Germany). The coordinates of the predefined target anatomy points were acquired using a neurosurgical navigation system (StealthStation Image Guidance Workstation; Medtronic, Dublin, Ireland) under direct visualization with the operating microscope and a 0° rigid endoscope (Karl Storz GmbH, Tüttlingen, Germany). The illustrative case was demonstrated retrospectively from the Burdenko Neurosurgery Center database. Provision of the clinical case was approved by the Burdenko Neurosurgery Center Ethics Board, and informed consent was obtained from the patient.

SIIS approach

The head was secured in a sitting position in this approach. A midline linear incision was made that extended from 2 cm above to 4 cm below the inion. A suboccipital craniotomy (3 × 5 cm) with the transverse sinus exposed as the superior boundary was performed. The dura was opened in a horseshoe fashion and tacked up toward the transverse sinus. In general, the trajectory of the approach starts 2.5 cm lateral from the midline at the craniotomy and goes deep over the superior cerebellar surface to the pineal gland, enters the

third ventricle, and then crosses to the contralateral side toward the body of the lateral ventricle [Figure 1].

Bridging veins can usually be preserved. The arachnoid membrane encountered in the quadrigeminal cistern is widely dissected to expose the vein of Galen and its tributaries. The superior vermian vein is always preserved by lateral mobilization. Once the galenic venous system and the pineal gland are identified, the arachnoid between the internal cerebral veins and pineal gland is dissected, and the third ventricle is accessed through the suprapineal recess.[16]

Further dissection proceeds with opening the inferior membrane of the tela choroidea, between the inferolateral wall of the contralateral internal cerebral vein and the medial surface of the thalamus [Figure 2a and Video 1]. Extending the approach along the superomedial surface of the thalamus permits identification of the choroidal fissure, which is located at the lateral margin of the roof of the third ventricle [Figure 2b]. Access of the body of the lateral ventricle requires perforation of the superior membrane of the tela choroidea and the tenia thalami [Figures 2c and d]. After the choroid plexus of the lateral ventricle is visualized, it is displaced medially toward the fornix to serve as a cushion of protection. The choroidal fissure is then enlarged gently by dynamic retraction of the fornix and the choroid plexus medially and the surface of the thalamus laterally using the microsurgical instruments [Figure 2e]. The tiny bridging arteries coursing from the posterior medial choroidal artery (PMChA) to the medial surface of the thalamus should be preserved if possible, but one small perforator could be sacrificed to increase the exposure of the body of the lateral ventricle. As the body of the lateral ventricle is entered, a 0° or 30° endoscope can be introduced to facilitate visualization of the intraventricular structures.

Quantitative measurements

First, seven points were identified on the exposed surface on the lateral ventricle to conceptualize the limits of the SIIS exposure
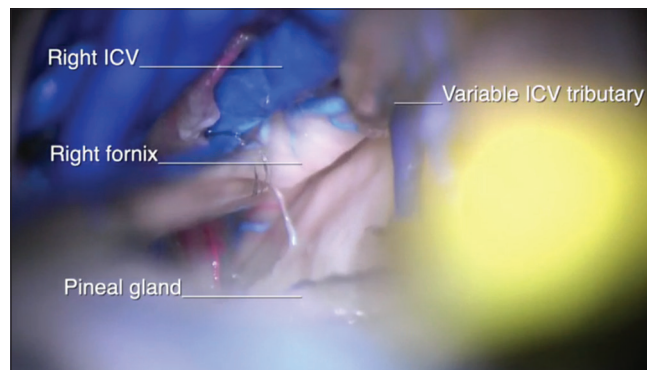
Video 1: Cadaveric video of the supracerebellar infratentorial inverted subchoroidal approach to the lateral ventricle. Used with permission from Barrow Neurological Institute, Phoenix, Arizona.
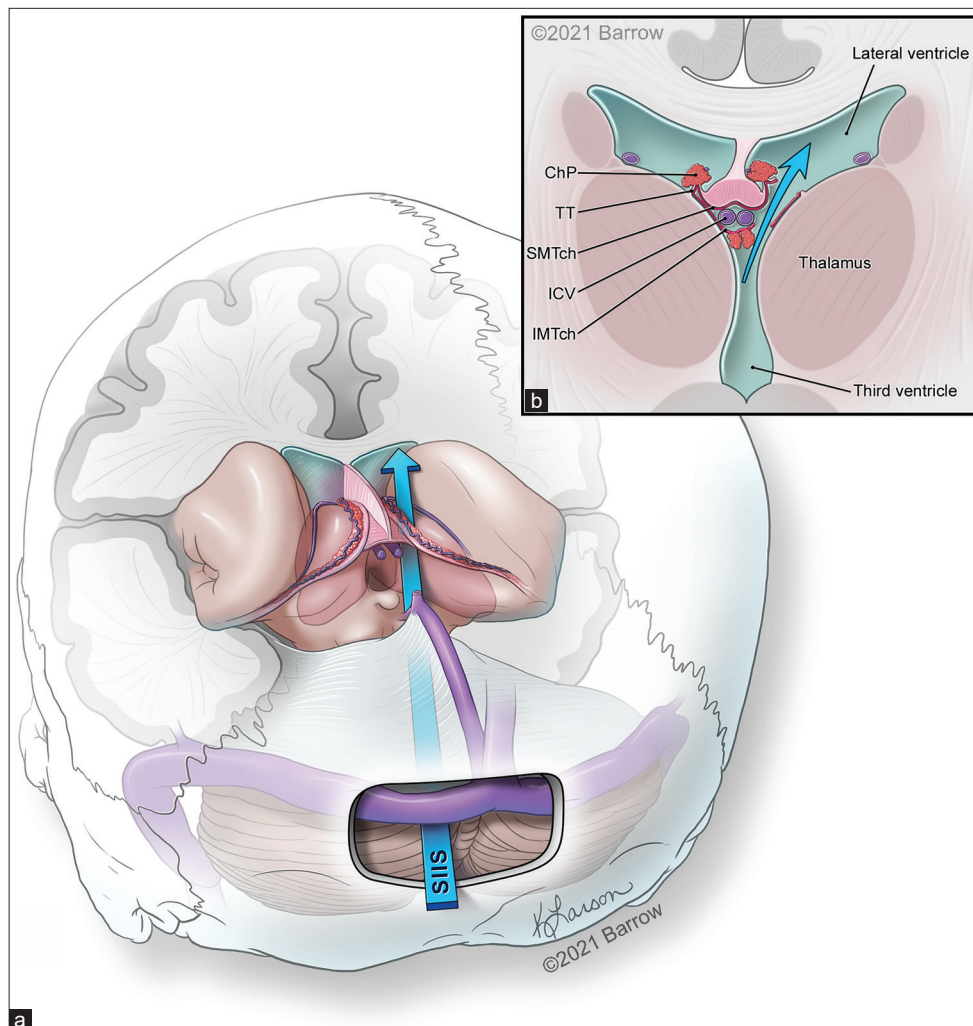
Figure 1: (a) Schematic illustration depicting the trajectory for the supracerebellar infratentorial inverted subchoroidal (SIIS) approach to the body of the lateral ventricle. (b) The SIIS approach is completed by an incision along the tenia thalami (TT). ChP: Choroid plexus, ICV: Internal cerebral vein, IMTch: Inferior membrane of the tela choroidea, SMTch: Superior membrane of the tela choroidea. Used with permission from Barrow Neurological Institute, Phoenix, Arizona.

[Figure 3a]. Their coordinates (x, y, and z) were recorded using the navigation system under direct operating microscopic (Points A-C) or 0° endoscopic (points D-G) visualization.

Point A, or the anterior choroidal point, was the most anterior reachable point on the floor of the lateral ventricle (thalamus) along the choroidal fissure; Point B, or the posterior choroidal point, was the most posterior reachable point on the floor (thalamus) of the lateral ventricle along the choroidal fissure; and Point C was the uppermost posterior reachable point on the lateral wall of the lateral ventricle. Points D and E were the most anterior reachable points on the junction of the medial wall and the roof and the junction of the lateral wall and the roof, respectively. Points F and G were the most posterior reachable points on the junction of the medial wall and the roof and on the junction of the lateral wall and the roof, respectively.

Furthermore, we established two constant coronal reference planes that corresponded to the anterior and posterior borders of the body of the lateral ventricle [Figure 3a]. These reference planes could be easily identified on MRI, and the extent of the exposure could be related to these two reference planes. The coordinates of the points that correspond to either reference plane on a cadaver were taken after the SIIS approaches measurements were obtained bilaterally.

The anterior coronal reference plane was defined by two points on the anterior margin of bilateral foramens of Monro (Points α_1 and α_3) and the point on the septum pellucidum (Point α_2), which was vertically superior to α_1 and α_3 and perpendicular to the imaginary line connecting them [Figures 3a and b].

The posterior coronal reference plane was located at the level where the crura of fornix and hippocampal formations fuse with the corpus callosum and where the septum pellucidum
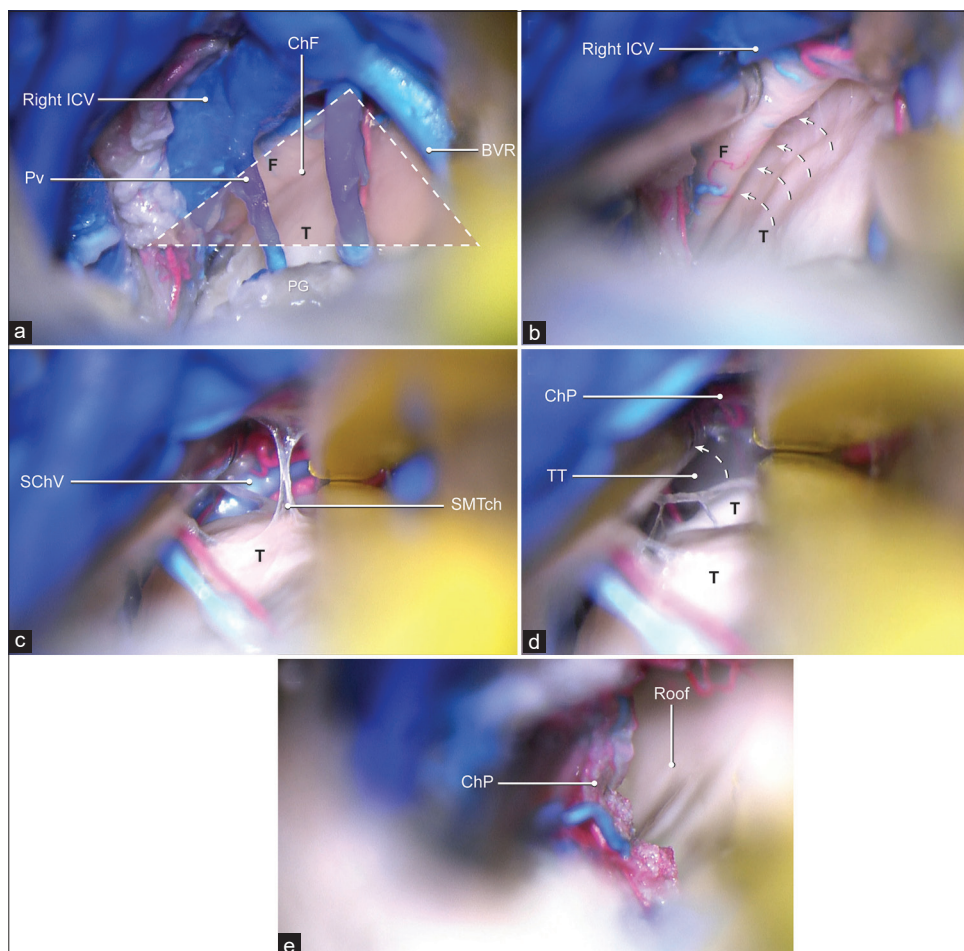
Figure 2: Stepwise description of the supracerebellar infratentorial inverted subchoroidal approach. (a) Inferior layer of the tela choroidea is removed. The trajectory to the choroidal fissure is surrounded by the pineal gland below, the contralateral internal cerebral vein, and the basal vein of Rosenthal laterally, which form a triangle (red area outlined with dashed lines). This triangular landmark can be used for identifying the initial dissection plane. (b) Once the tela choroidea is entered, extending the approach along the superomedial surface of the thalamus permits identification of the choroidal fissure, which is located between the contralateral fornix and thalamus. The contralateral fornix is then retracted medially (dashed arrows) to widen the choroidal fissure. (c) The choroid plexus of the lateral ventricle is identified after the superior membrane of the tela choroidea is dissected, with the fornix displaced medially. (d) To access the cavity of the lateral ventricle, the choroid plexus is displaced medially (dashed arrow) and the tenia thalami is penetrated. (e) The intraventricular cavity is exposed. BVR: Basal vein of Rosenthal, ChF: Choroidal fissure, ChP: Choroid plexus, F: Fornix, ICV: Internal cerebral vein, PG: Pineal gland, Pv: Pineal vein, Roof: Roof of the lateral ventricle, SChV: Superior choroidal vein, SMTch: Superior membrane of the tela choroidea, T: Thalamus, TT: Tenia thalami. Used with permission from Barrow Neurological Institute, Phoenix, Arizona.

disappears. The points taken to define this plane included two points on the lateral margins of the left and right crus of fornix (Points β_1 and β_3) and one point on the junction of the corpus callosum and septum pellucidum (Point β_2), which was vertically superior to β_1 and β_3 and perpendicular to the imaginary line connecting them [Figures 3a and c]. We then established the equation of both reference planes by solving the three equations using the three predefined points to calculate *a, b, c,* and *d,* using the plane equation formula *ax + by + cz + d = 0.*

The coordinates obtained were used for calculating the distances between the points on the surfaces of the lateral ventricle and for assessing the horizontal distance from these points to the reference planes: from Points A, D, and E to the anterior plane and from Points B, C, F, and G to the posterior plane. We measured the length of exposure along the choroidal (from Point A to Point B), the working distances at the anterior limit of exposure (from Point A to Points D and E) and at the posterior limit of exposure (from Point B to Points C, F, and G), and the surgical depth from the craniotomy window and the anterolateral limit of exposure on the roof of the lateral ventricle (Point E). Point E was used because it represented the most anteriorly situated point in the ventricle.
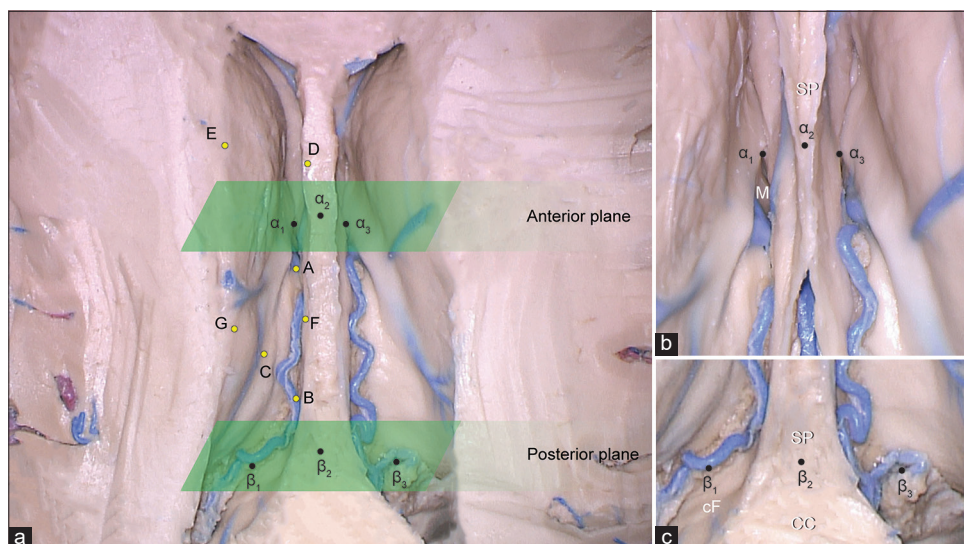
Figure 3: (a) Photograph of cadaveric dissection showing the lateral ventricles. The roof of the lateral ventricle is removed. The approximate trajectory of the supracerebellar infratentorial inverted subchoroidal (SIIS) approach is depicted with the positions of seven yellow points (A-G) inside each ventricle that define the area of exposure. A is the most anterior reachable point on the floor of the lateral ventricle along the choroidal fissure, B is the most posterior reachable point on the floor of the lateral ventricle along the choroidal fissure, C is the uppermost posterior reachable point on the lateral wall, D is the most anterior reachable point on the junction of the medial wall and the roof of the lateral ventricle, E is the most anterior reachable point on the junction of the lateral wall and the roof of the lateral ventricle, F is the most posterior reachable point on the junction of the medial wall and the roof of the lateral ventricle, and G is the most posterior reachable point on the junction of the lateral wall and the roof of the lateral ventricle. The planes corresponding to the anterior and posterior margins of the body of the lateral ventricle are depicted with green parallelograms. Enlarged view of the anterior (b) and posterior (c) margins of the body of the lateral ventricle with the position of points that correspond to the anterior and posterior planes. α_1 is the point on the anterior margin of left foramen of Monro, α_3 is the point on the anterior margin of right foramen of Monro, α_2 is the point on the septum pellucidum, β_1 is the point on the lateral margin of the left crus of the fornix, β_3 is the point on the lateral margin of the right crus of the fornix, β_2 is the point on the junction of the corpus callosum and septum pellucidum. CC: Corpus callosum, cF: Crus fornix, M: Foramen of Monro, SP: Septum pellucidum. Used with permission from Barrow Neurological Institute, Phoenix, Arizona.

The distances (in millimeters) between each exposed point on the ventricular surface and the reference planes were calculated using the following formula:

$$Distance = \left| \frac{ax_0 + by_0 + cz_0 + d}{\sqrt{a^2 + b^2 + c^2}} \right| \qquad (1)$$

where a, b, c, and d are the coefficients that characterize the equation of a reference plane and x_0, y_0, and z_0 are the coordinates of the identified point on the ventricular surface.

Statistical analysis

Surgical depth and distances were calculated using Microsoft Excel 2013 (Microsoft Corp., Redmond, WA) and are presented as mean and standard deviation (SD). Statistical analysis was performed using GraphPad Prism 5 (GraphPad Software, Inc., La Jolla, CA). The Spearman correlation coefficient was used to assess the associations between two continuous variables. $P < 0.05$ was considered statistically significant.

RESULTS

Anatomy observation of the lateral ventricle through the SIIS approach

The lateral ventricular cavity was explored via the operating microscopic and 30° and 0° endoscopic views alternately [Figures 4 and 5]. The first structure that came into the microscopic view following the choroidal fissure exposure was the caudate nucleus, then the roof of the lateral ventricle could be visualized, which lies behind and superior to the caudate nucleus [Figure 4a]. The venous angle was the anatomical structure that limited the choroidal fissure dissection anteriorly in all dissections [Figures 4b and c]. This classic venous angle is formed by the thalamostriate, internal cerebral, and anterior septal veins.[10] The anatomical structure that limited the choroidal fissure dissection posteriorly was the thalamocaudate vein in all specimens [Figures 4d and e]. Although we used both the operating microscope and the endoscopic assistance to determine the limits of the exposure for the quantitative analysis, the endoscope provided significantly larger in-focus visualized area in terms of inspection.
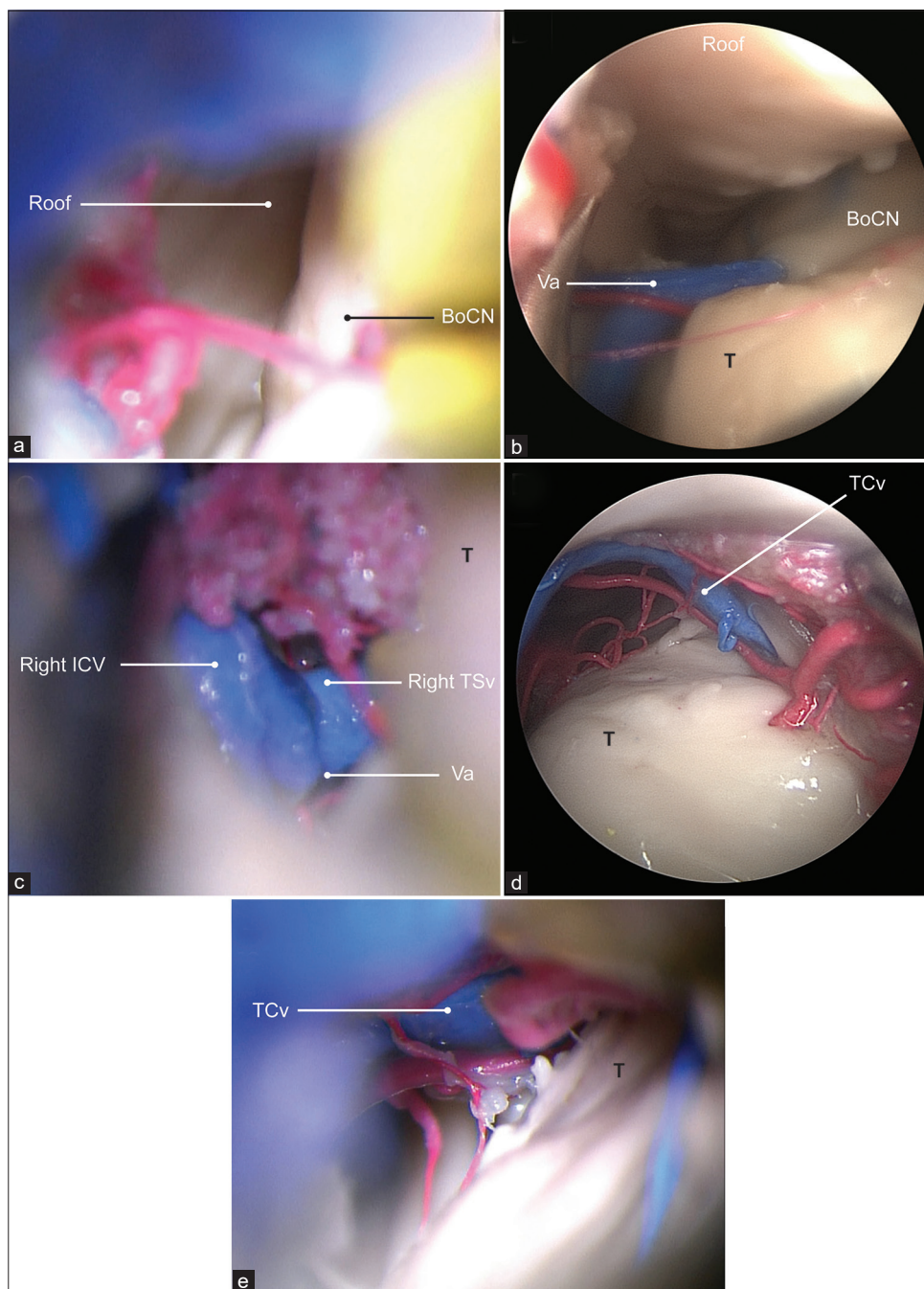
Figure 4: (a) The lateral ventricle is exposed in its posterior aspect under the operating microscope. (b) A 0° endoscopic view showing the anterior limiting structure of the approach from the venous angle. (c) Microscopic view showing the anterior limiting structure of the approach from the venous angle. (d) A 0° endoscopic view showing the posterior limiting structure of the approach from the thalamocaudate vein. (e) Microscopic view showing the posterior limiting structure of the approach. BoCN: Body of the caudate nucleus, ICV: Internal cerebral vein, Roof: Roof of the lateral ventricle, T: Thalamus, TCv: Thalamocaudate vein, TSv: Thalamostriate vein, Va: Venous angle. Used with permission from Barrow Neurological Institute, Phoenix, Arizona.

Quantitative analysis of the exposed area

The mean accessible length of the choroidal fissure through the SIIS approach, which was defined as a distance between Points A and B, was 19 (3.1) mm.

Point A was located 7 (5.1) mm posteriorly to the anterior plane, whereas Point B was located 8 (3.0) mm anterior to the posterior plane.

Points D and E (the most anterior reachable points on the junction between the roof and the medial and lateral walls) were
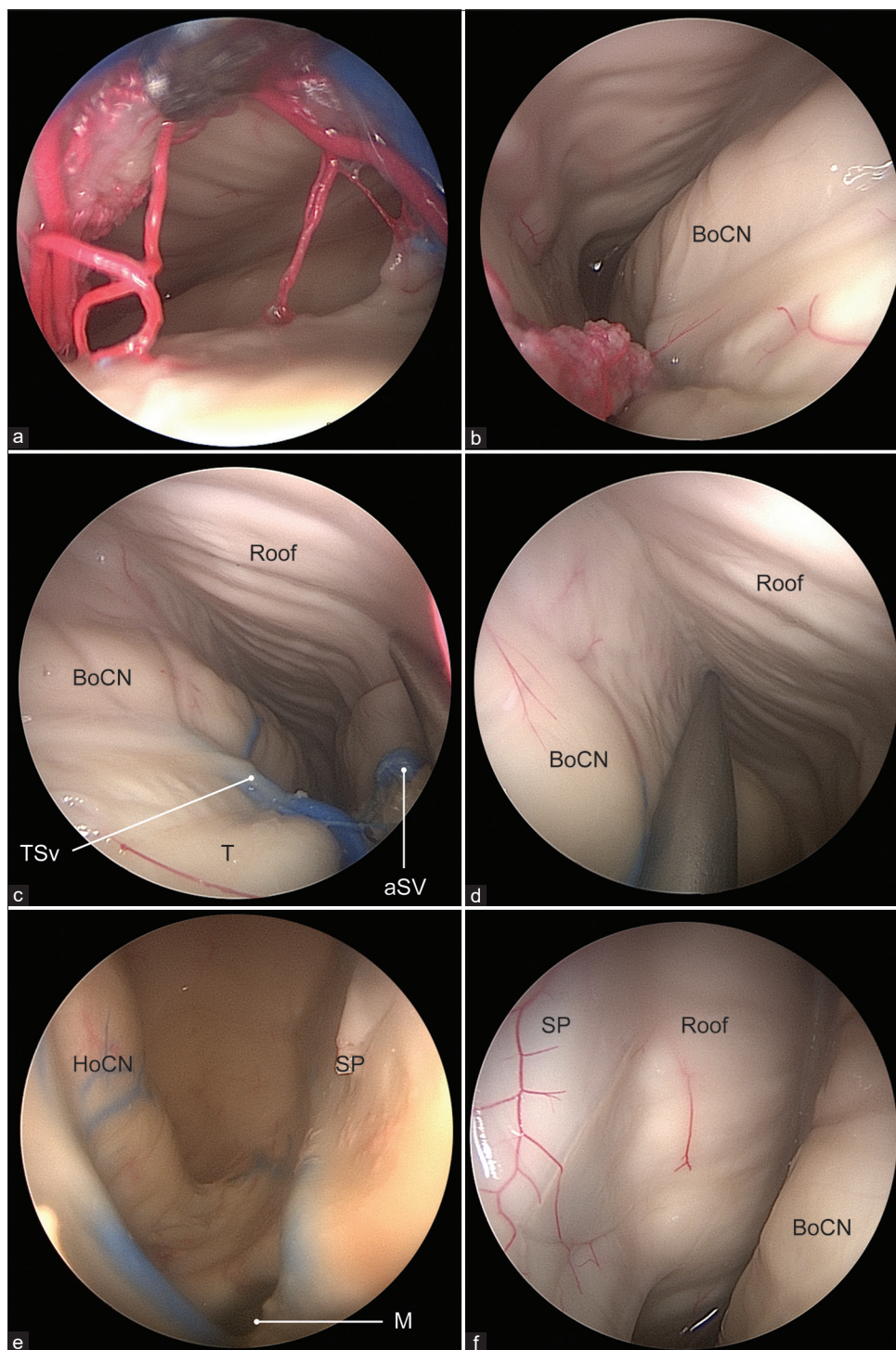
Figure 5: (a) A 0° endoscopic view of the entrance to the posterior aspect of the body of the lateral ventricle. (b) The walls of the lateral ventricle can be clearly identified. A 0° endoscopic views of the entrance to the anterior aspect of the body of the lateral ventricle and the trajectory to the junction of the roof with the medial (c) and lateral (d) walls. The foramen of Monro (e) and septum pellucidum (f) are clearly visualized with the 30° endoscope. aSV: Anterior septal vein, BoCN: Body of the caudate nucleus, HoCN: Head of the caudate nucleus, M: Foramen of Monro, Roof: Roof of the lateral ventricle, SP: Septum pellucidum, T: Thalamus, TSv: Thalamostriate vein. Used with permission from Barrow Neurological Institute, Phoenix, Arizona.

9 (7.0) mm and 11 (5.8) mm anterior to the anterior reference plane, respectively. Point F (the most posterior reachable point on the roof and medial wall) was 17 (9.2) mm anterior to the posterior reference plane, whereas Point G (the most posterior

reachable point on the roof and lateral wall) was 15 (9.2) mm anterior to the posterior reference plane. Point C was 9 (7.2) mm anterior to the posterior reference plane. The distance from the craniotomy window to Point E was 109 (17.0) mm.
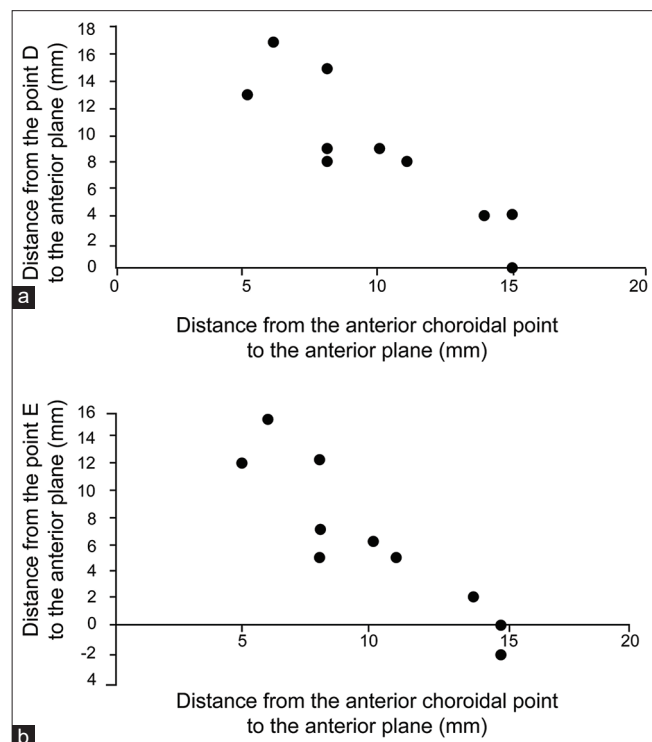
The distances from the anterior choroidal point (Point A) to the anterior reference plane had a strong negative correlation with the distances from the most anterior reachable points (Points D and E) to the anterior reference plane ($r = -0.87$, $P < 0.001$; $r = -0.92$, $P < 0.001$; respectively) [Figures 6a and b].

However, there was no significant correlation between the distances of the posterior reachable Points F and G and posterior choroidal point (Point B) to the posterior reference plane ($r = 0.52$, $P = 0.11$; $r = 0.57$, $P = 0.08$; respectively).

The mean distances from the anterior choroidal point to Points D and E were 21 (7.6) mm and 23 (6.6) mm, respectively. The mean distances from the posterior choroidal point to Points F, G, and C were 18 (7.5) mm, 19 (9.1) mm, and 5 (3.3) mm, respectively.

Illustrative case

Among several unique cases supporting this study, the clinical application of the SIIS approach is illustrated by

Figure 6: (a) The relationship between the distances from the anterior choroidal point and Point D to the anterior plane in millimeters. (b) The relationship between the distances from the anterior choroidal point and Point E to the anterior plane in millimeters. Used with permission from Barrow Neurological Institute, Phoenix, Arizona.

a clinical case performed by one of the authors (D.P.). A 42-year-old man with a history of colon adenocarcinoma was referred to the specialized neurosurgical center from an outside hospital with headache, episodes of vomiting, gait ataxia, and imbalance. MRI revealed separate brain lesions in the fourth ventricle and right lateral ventricle [Figures 7a-d]. The fourth ventricular mass compressed the brainstem and was interpreted with impending cerebrospinal fluid (CSF) flow interruption. The stage of the colon cancer was not exactly designated, but the patient had been without active disease for years. No other metastases were determined by positron emission tomography or other related scanning. Systemic therapy for adenocarcinoma status and testing for tumor markers were unknown. A suboccipital craniotomy was performed with the patient in a sitting position that exposed the foramen magnum and transverse sinus and a telovelar approach to the fourth ventricle was performed to remove the inferiorly located lesion. The tumor invaded the floor of the fourth ventricle. Intraoperative biopsy had inconclusive results and the differential diagnosis included medulloblastoma and primary CNS lymphoma (PCNSL). Given the patient's history of adenocarcinoma and the location of the lateral ventricle tumor, as well as the fact that its imaging characteristics did not resemble those of a typical PCNSL, resection of the second lesion proceeded to obtain tissue to provide guidance for postoperative adjuvant therapy.

An SIIS approach to the right lateral ventricle was performed through the same craniotomy [Figures 7e and f]. Dissection of the choroidal fissure allowed identification of the lesion arising from the dorsal surface of the thalamus [Figure 7g]. The pattern of tumor invasion in the surrounding brain was similar to that of the fourth ventricular lesion. Portions of the tumor were removed with bipolar coagulation and suction. Inspection of the lateral ventricle revealed residual tumor in the posterolateral part of the body of the lateral ventricle; this part appeared to be inaccessible through this approach. The postoperative period was uneventful, and the patient was discharged on postoperative day 7. The postoperative MRI demonstrated residual of the second lesion [Figures 7h-j]. Retrospective application of the devised predicting system of the SIIS approach to this case indicated that the posterior portion of the tumor did not appear to be fully accessible [Figure 8]. The final pathology diagnosis was consistent with PCNSL, and the patient began adjuvant intra-arterial and intravenous chemotherapy.

DISCUSSION

Anatomical considerations of the SIIS approach

Despite the progress in modern neurosurgery, intraventricular tumors remain among the most difficult to approach. With currently available approaches, it is impossible to reach the lateral ventricle without transgressing the corpus callosum or cerebral cortex. Although the transcortical and
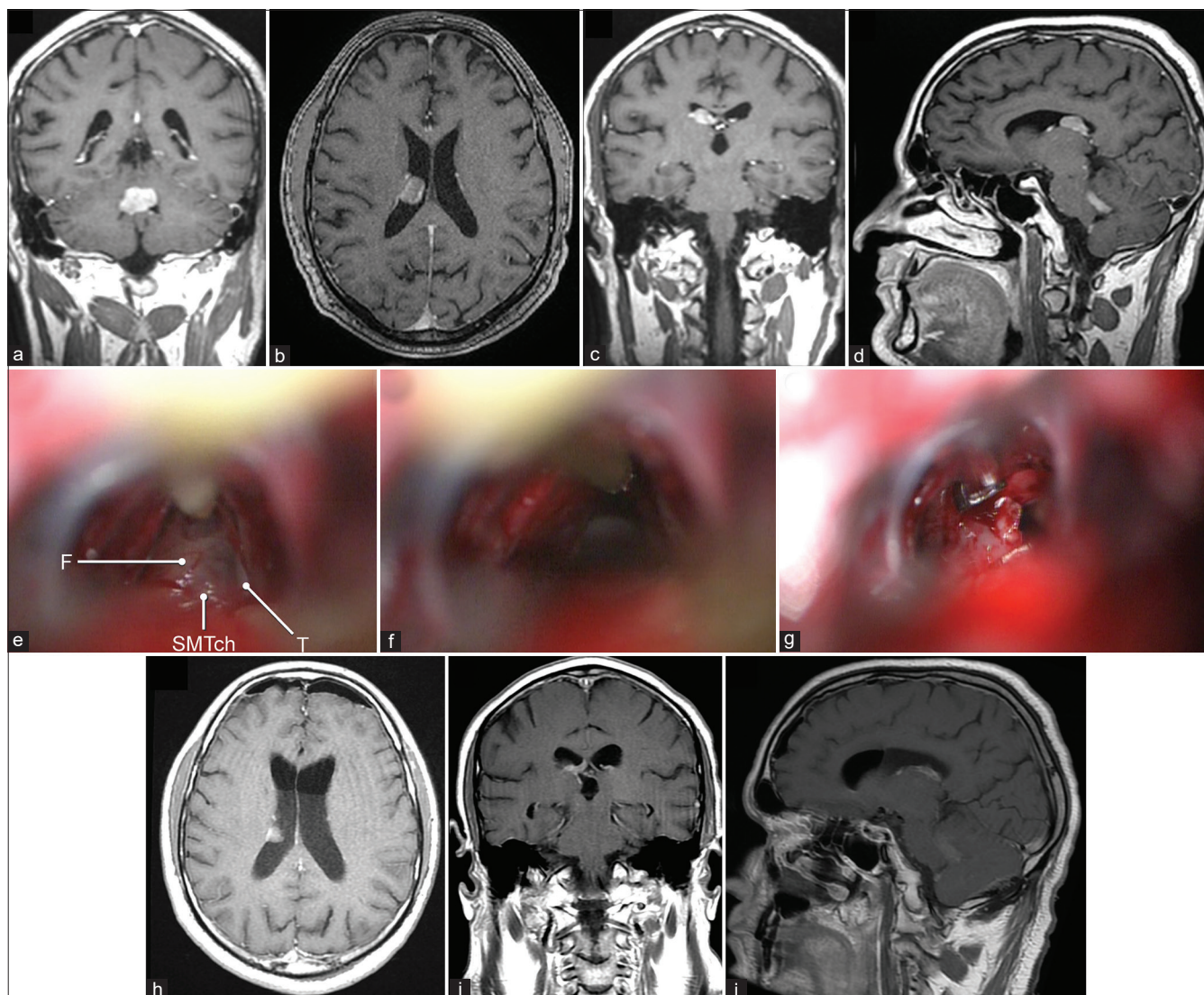
Figure 7: (a) Preoperative T1-weighted contrast-enhanced magnetic resonance imaging (MRI) in coronal view showing heterogeneous enhancing lesions in the fourth ventricle. Axial (b), coronal (c), and sagittal (d) views showing heterogeneous enhancing lesion in the right lateral ventricle. (e) Intraoperative photograph showing microsurgical dissection of the roof of the third ventricle. (f) Dissection of the roof of the third ventricle enables access to the right lateral ventricle. (g) Intraoperative photograph of tumor resection through the supracerebellar infratentorial inverted subchoroidal approach. Axial (h), coronal (i), and sagittal (j) postoperative T1-weighted MRIs with contrast showing residual tumor left in the posterolateral part of the lateral ventricle. F: Fornix, SMTch: Superior membrane of the tela choroidea, T: Thalamus. Used with permission from Barrow Neurological Institute, Phoenix, Arizona.

interhemispheric transcallosal approaches could be performed through relatively small incisions, damage of the normal brain tissue could result in neurological deficits.[2,14,18,20] Here, we described a novel SIIS approach that provides access to the body of the lateral ventricle through natural fissures without transgression of the brain tissue.

The SIIS approach is a contralateral approach, with an optimal starting point located about 2.5 cm off the midline. The trajectory of SIIS is directed upward through the supracerebellar infratentorial space, crosses the midline

anterior to the pineal gland in the third ventricle, and enters the contralateral lateral ventricle through the choroidal fissure at the roof of the third ventricle.

The initial step in performing this approach is the dissection of the roof of the third ventricle. Due to the natural compactness of this area, finding the right plane of dissection that would lead to the lateral ventricle can be difficult. Dissecting the roof of the third ventricle without direct visualization of the body of the fornix risks damage to the fornix. At this stage, an anatomical triangle could be used as
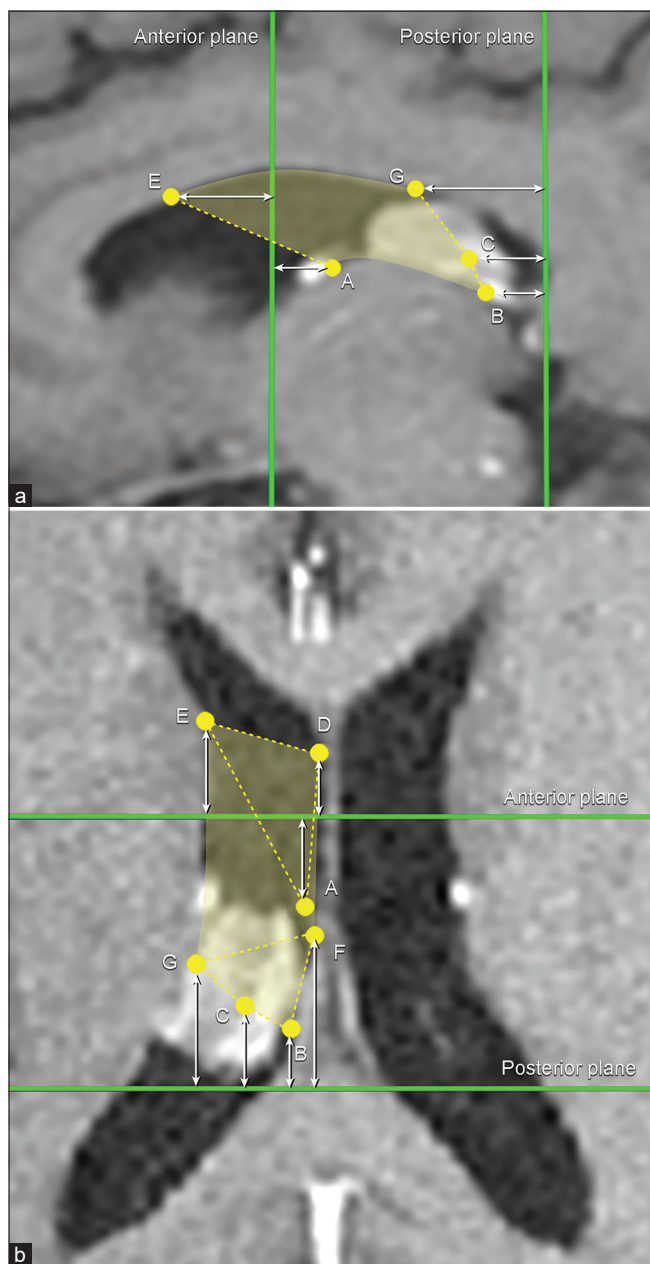
Figure 8: Application of the preoperative predictive system for the planning of the supracerebellar infratentorial inverted subchoroidal (SIIS) approach on the preoperative sagittal (a) and axial (b) views. The anterior and posterior limits of the approach (dashed yellow lines) are defined after applying the mean distances (double arrows) from the anterior and posterior exposures of the approach to the anterior and posterior planes. Points E and D are a mean (SD) of 11 (5.8) mm and 9 (7.0) mm anterior to the anterior plane, respectively, and Point A is 7 (5.1) mm posterior to the anterior plane. Points G, C, B, and F are a mean (SD) of 15 (9.2) mm, 9 (7.2) mm, 8 (3.0) mm, and 17 (9.2) mm anterior to the posterior plane, respectively. The area of exposure in the lateral ventricle with the SIIS approach is highlighted in yellow. The anterior and posterior planes are depicted with solid green lines. The posterior part of the tumor lying posterior to the posterior limit of the approach appears to be difficult to access. Used with permission from Barrow Neurological Institute, Phoenix, Arizona.

a landmark for orientation to deepen the initial dissection trajectory from the third ventricle toward the choroidal fissure. This triangle is formed by the contralateral internal cerebral vein above, contralateral basal vein of Rosenthal posterolaterally, and the pineal gland below [Figure 2a].

Further dissection proceeds between the perforators of the PMChA and branches of the internal cerebral veins. It is usually necessary to sacrifice some of these vessels when the third ventricle is approached through the classic subchoroidal approach.[25] However, with extreme care, the PMChA perforators can be preserved while manipulating between them.

The SIIS approach is directed through the thalamic side of the choroidal fissure, leaving the attachment of the choroid plexus to the fornix undisturbed. Therefore, the fornix remains covered by the choroid plexus, which reduces impingement to the fornix while manipulating within the lateral ventricle.

Endoscopic assistance with straight and angled-view endoscopes could improve the visualization of the intraventricular space, which is mostly hidden when viewing through this narrow and deep approach using the operating microscope [Figures 5e and f].

Prediction system to estimate the area of exposure

By performing a quantitative anatomical investigation of the SIIS approach, we developed a system that could be used to estimate the area of exposure within the lateral ventricle on the basis of the preoperative MRI and to predict whether a lesion can be accessed through this approach. Such a system could be used for preoperative planning and approach selection. This predictive system involves the assessment of the limits of the lateral ventricle lesion in relation to the anterior and posterior reference planes and the assessment of the approach-limiting anatomical structures.

The rationale defining the reference planes was to select constant planes associated with easily identifiable anatomical landmarks from MRI. The anterior reference plane corresponds to the coronal plane through the anterior margin of the foramen of Monro, whereas the posterior reference plane corresponds to the posterior margin of the body of the lateral ventricle [Figures 3a-c and 7e].[24]

Following the establishment of two planes on MRI, the limits of anterior and posterior exposure as well as the choroidal fissure opening could be identified using the obtained measurements. Our results showed the anterior exposure on the medial and lateral margins of the roof of the lateral ventricle were 9 (7.0) mm (Point D) and 11 (5.8) mm (Point E) anterior to the anterior plane, and the anterior choroidal point (Point A) was 7 (5.1) mm posterior to it. The anterior working distances, which were defined as AD and AE,

estimate the anterior limit of the exposure through the SIIS approach; tumors arising anterior to this limit are deemed to be inaccessible in the anterior part of the lateral ventricle. The same measurements were made in relation to the posterior exposure; thus, tumors that are located posterior to the posterior working distance (BC, BF, and CG) would be challenging to remove. This observation was retrospectively confirmed by the illustrative case.

Finally, variations in the normal anatomical structures should also be considered for planning the SIIS approach. The major limiting factor of the anterior limits of the choroidal fissure dissection is the venous angle formed by the junction of the anterior septal, thalamostriate, and internal cerebral veins. The importance of the venous angle variations in surgical procedures involving the lateral and third ventricles has been reinforced.[7] Our data were shown to be consistent with this anatomy, because the anterior limit of the exposure was correlated with the location of the venous angle. The more posteriorly the venous angle is located, the less anterior exposure can be achieved. However, tumors extending anteriorly to the frontal horn can be approached through both the SIIS approach and the foramen of Monro. Although the location of the thalamocaudate vein (the posterior limit during dissection of the choroidal fissure) did not affect the posterior extent of the SIIS approach in the lateral ventricle, consideration of its anatomical position is still crucial.

Limitations of the SIIS approach

The main limitation of the SIIS approach is the narrow working space through a number of important surrounding neurovascular structures (e.g., the fornix, internal cerebral veins, and choroidal arteries). Although the surgical corridor is established by dissections along the natural fissures, the depth and narrowness of the approach require utmost caution during surgical manipulations. According to the anatomical assessment, lesions extending to the anterior portion of the frontal horn or the atrium of the lateral ventricle could not be fully accessed through the SIIS approach.

Clinical application

Selecting an appropriate patient who would benefit from the SIIS approach, compared with other approaches to the lateral ventricle, requires careful considerations. The interhemispheric and transcortical approaches are relatively safe and efficient approaches for sole lateral ventricular lesions.[1,9,17] However, these approaches cannot address posterior fossa lesions from the same craniotomy.

The SIIS approach is better suited for patients with familial cavernous malformations and multiple symptomatic lesions, including tumors. Our case example demonstrated a patient with multiple brain tumors, and these patients are thought

to have a worse overall survival compared with patients with one lesion.[19,21] Deciding whether a patient with multiple intracranial tumors is a good surgical candidate includes assessment of multiple factors, including the number of lesions, their radiological features, previous histology findings (if known), control of the extracranial diseases, and the patient's overall health status. For example, patients with one to four accessible or life-threatening metastases without systemic disease may be considered for surgery.[4,5] However, in patients with multiple brain tumors, after the histologic diagnosis is established, postoperative adjuvant therapy is preferred when possible.

In carefully selected cases, the SIIS approach can be used to simultaneously remove multiple tumors located in the upper cerebellum, the pineal region, and the body of the lateral ventricle via the same craniotomy. It can also be combined with a telovelar approach, because both approaches require a midline incision and a suboccipital craniotomy in the same area. Therefore, some multiple lesions that would otherwise require a staged procedure or separate craniotomies when approaching supra- and infratentorial compartments could be accessed during a single procedure with the SIIS approach if the case is selected carefully.

In our clinical case, both tumors represented solid masses and given the history of no previous neurosurgical disease, but history of colon adenocarcinoma and imaging characteristics, these lesions were initially considered as metastases. However, to establish a proper treatment strategy, confirmation of the nature of the pathology was paramount. Considering the eloquent location of the fourth ventricle tumor, a decision was made to remove it and restore CSF flow. The preoperative strategy centered on verification of the nature of the fourth ventricle tumor that would further prompt probable assignment of radiosurgery for the lateral ventricle lesion.

Despite the expectations, the intraoperative biopsy of the fourth ventricle tumor was interpreted as a PCNSL or medulloblastoma, and thus more perplexity than clarity arose in the case. The pattern of pathology of the tumor infiltrating the fourth ventricle more closely resembled a PCNSL. Intraventricular PCNSLs are extremely rare, with only a few cases of simultaneous involvement of the fourth and lateral ventricles described.[27] Therefore, considering a low prevalence of PCNSLs inside the ventricles and the imaging characteristics of the lateral ventricle tumor not resembling PCNSL, an SIIS approach was performed to resect the tumor. Confirmation of the nature of the lateral ventricle tumor was also mandatory to exclude or confirm activation of previously silent colon cancer. Another option to consider as a second-stage procedure for the lateral ventricle tumor would be stereotactic or endoscopic biopsy. Although in patients with small ventricles, these procedures can be associated with

unnecessary damage to the deep brain structures or bleeding that can result in significant morbidity.[6,12,22,29] For this specific case, it may be argued that once PCNSL was established from the posterior fossa lesion, the risk of advancing into the lateral ventricle from this approach outweighs the benefit of resecting the second lesion given the literature on PCNSL responsiveness to chemotherapy and radiation. However, given with the history of adenocarcinoma and the rarity of the multiply located PCNSL, the strategy for approach seems justified.

Surgical removal of multiple brain tumors simultaneously in patients who are candidates for further adjuvant therapy can affect their long-term prognosis, especially in patients with lesions located in the safe resection areas, or in cases of rare lesions. Such a surgical strategy might be feasible in patients with highly radioresistant tumors or those who undergo chemotherapy that causes significant cerebral edema.[13,30] In one study, no difference was shown in terms of risks of mortality between removing multiple brain lesions and one solitary lesion.[5] Compared with the two-step surgical procedure, the single-stage surgery in patients with multiple brain tumors and with newly diagnosed or active systemic disease may decrease the overall risk of prolonged hospitalization for multiple surgeries and avoid delay in adjuvant therapy.

Study limitations

One of the drawbacks of this study is the inherent bias related to the stiffness of the cadaver brain tissue. The study used selected anatomical reference points that may be subject to variation and prone to shift during live surgery on entering the basal cisterns or ventricular system. The release of CSF or its redistribution in these situations may lead to difficulty in achieving a reliable or accurate navigation.

Quantification of this approach by this study did not necessarily confirm its superiority over the two standard tandem approaches (i.e., infratentorial supracerebellar approach, followed by minimally invasive frontal microsurgical or endoscopic approach). However, although the SIIS is challenging, it represents an alternative workable and successful surgical avenue.

The dynamic manipulation of the fornix, perforators, and deep venous system is not without consequences. The deep venous system may show variation, its integrity is of paramount importance, and its compromise may lead to unpredicted catastrophic outcomes. Furthermore, variations in the ventricle size could affect the measurement results and introduce bias. For example, the anterior and posterior limits of the exposure were greater in specimens with enlarged ventricles, rather than in those with small ventricles. The large SDs of some measurements were likely attributable to the variable size of the ventricles in the examined specimens and anatomical

variability. Nevertheless, we believe that this anatomical study provides valuable insight into the feasibility and assessment of the SIIS within a controlled laboratory setting.

CONCLUSION

The described SIIS approach can accomplish simultaneous resection of multiple brain lesions arising in the posterior fossa, the pineal region, and the body of the lateral ventricle. The SIIS approach is more favorable for reaching lesions that do not extend to the anterior part of the frontal horn of the ventricle or posterior to the atrium. Endoscopic assistance is essential when exploring the ventricle, because the endoscope provides a high-quality magnified view in a flexible direction that cannot be offered by a microscope. However, the desire of the surgeon to achieve total resection of multiple brain tumors should not expose the patient to a greater risk of postoperative morbidity, and each case requires unique preoperative consideration. Such an approach is a complex, difficult corridor that demands thoroughly expert anatomical familiarity, and thus is the rationale for our exposure estimation and predictive system.

Declaration of patient consent

The authors certify that they have obtained all appropriate patient consent.

Conflicts of interest

There are no conflicts of interest.

REFERENCES

1. Abla AA, Spetzler RF, Albuquerque FC. Trans-striatocapsular contralateral interhemispheric resection of anterior inferior basal ganglia cavernous malformation. World Neurosurg 2013;80:e397-9.
2. Aryan HE, Ozgur BM, Jandial R, Levy ML. Complications of interhemispheric transcallosal approach in children: Review of 15 years experience. Clin Neurol Neurosurg 2006;108:790-3.
3. Baker CM, Glenn CA, Briggs RG, Burks JD, Smitherman AD, Conner AK, *et al*. Simultaneous resection of multiple metastatic brain tumors with multiple keyhole craniotomies. World Neurosurg 2017;106:359-67.
4. Bindal AK, Bindal RK, Hess KR, Shiu A, Hassenbusch SJ, Shi WM, *et al*. Surgery versus radiosurgery in the treatment of brain metastasis. J Neurosurg 1996;84:748-54.
5. Bindal RK, Sawaya R, Leavens ME, Lee JJ. Surgical treatment of multiple brain metastases. J Neurosurg 1993;79:210-6.
6. Cheng G, Yu X, Zhao H, Cao W, Li H, Li Q, *et al*. Complications

of stereotactic biopsy of lesions in the sellar region, pineal gland, and brainstem: A retrospective, single-center study. Medicine (Baltimore) 2020;99:e18572.

7. Cimşit NC, Türe U, Ekinci G, Pamir MN, Erzen C. Venous variations in the region of the third ventricle: The role of MR venography. Neuroradiology 2003;45:900-4.

8. Dagenais GR, Leong DP, Rangarajan S, Lanas F, Lopez-Jaramillo P, Gupta R, *et al*. Variations in common diseases, hospital admissions, and deaths in middle-aged adults in 21 countries from five continents (PURE): A prospective cohort study. Lancet 2020;395:785-94.

9. Ellenbogen RG. Transcortical surgery for lateral ventricular tumors. Neurosurg Focus 2001;10:E2.

10. Fujii S, Kanasaki Y, Matsusue E, Kakite S, Kminou T, Ogawa T. Demonstration of cerebral venous variations in the region of the third ventricle on phase-sensitive imaging. AJNR Am J Neuroradiol 2010;31:55-9.

11. Gazzeri R, Nalavenkata S, Teo C. Minimally invasive key-hole approach for the surgical treatment of single and multiple brain metastases. Clin Neurol Neurosurg 2014;123:117-26.

12. Grunert P, Hopf N, Perneczky A. Frame-based and frameless endoscopic procedures in the third ventricle. Stereotact Funct Neurosurg 1997;68:80-9.

13. Guirguis LM, Yang JC, White DE, Steinberg SM, Liewehr DJ, Rosenberg SA, *et al*. Safety and efficacy of high-dose interleukin-2 therapy in patients with brain metastases. J Immunother 2002;25:82-7.

14. Jeeves MA, Simpson DA, Geffen G. Functional consequences of the transcallosal removal of intraventricular tumours. J Neurol Neurosurg Psychiatry 1979;42:134-42.

15. Johnson JD, Young B. Demographics of brain metastasis. Neurosurg Clin N Am 1996;7:337-44.

16. Konovalov AN, Pitskhelauri DI. Infratentorial supracerebellar approach to the colloid cysts of the third ventricle. Neurosurgery 2001;49:1116-22; discussion 1122-3.

17. Lawton MT, Golfinos JG, Spetzler RF. The contralateral transcallosal approach: Experience with 32 patients. Neurosurgery 1996;39:729-34; discussion 734-5.

18. Milligan BD, Meyer FB. Morbidity of transcallosal and transcortical approaches to lesions in and around the lateral and third ventricles: A single-institution experience. Neurosurgery 2010;67:1483-96; discussion 1496.

19. Mintz AH, Kestle J, Rathbone MP, Gaspar L, Hugenholtz H, Fisher B, *et al*. A randomized trial to assess the efficacy of surgery in addition to radiotherapy in patients with a single cerebral metastasis. Cancer 1996;78:1470-6.

20. Nakasu Y, Isozumi T, Nioka H, Handa J. Mechanism of mutism following the transcallosal approach to the ventricles. Acta Neurochir (Wien) 1991;110:146-53.

21. Nieder C, Astner ST, Grosu AL, Andratschke NH, Molls M. The role of postoperative radiotherapy after resection of a single brain metastasis. Combined analysis of 643 patients. Strahlenther Onkol 2007;183:576-80.

22. Oka K, Yamamoto M, Nagasaka S, Tomonaga M. Endoneurosurgical treatment for hydrocephalus caused by intraventricular tumors. Childs Nerv Syst 1994;10:162-6.

23. Paek SH, Audu PB, Sperling MR, Cho J, Andrews DW. Reevaluation of surgery for the treatment of brain metastases: Review of 208 patients with single or multiple brain metastases treated at one institution with modern neurosurgical techniques. Neurosurgery 2005;56:1021-34; discussion 1021-34.

24. Rhoton AL Jr. The lateral and third ventricles. Neurosurgery 2002;51 Suppl 4:S207-71.

25. Rhoton AL Jr., Yamamoto I, Peace DA. Microsurgery of the third ventricle: Part 2. Operative approaches. Neurosurgery 1981;8:357-73.

26. Stark AM, Tscheslog H, Buhl R, Held-Feindt J, Mehdorn HM. Surgical treatment for brain metastases: Prognostic factors and survival in 177 patients. Neurosurg Rev 2005;28:115-9.

27. Suri V, Mittapalli V, Kulshrestha M, Premlani K, Sogani SK, Suri K. Primary intraventricular central nervous system lymphoma in an immunocompetent patient. J Pediatr Neurosci 2015;10:393-5.

28. Tanei T, Fujii M, Takebayashi S, Nakahara N, Wakabayashi T. Simultaneous multiple craniotomies in the management of multifocal malignant brain lesions: Case reports. Fukushima J Med Sci 2019;65:43-9.

29. Torrens MJ. Endoscopic neurosurgery. Neurosurg Q 1995;5:18-33.

30. Yaeh A, Nanda T, Jani A, Rozenblat T, Qureshi Y, Saad S, *et al*. Control of brain metastases from radioresistant tumors treated by stereotactic radiosurgery. J Neurooncol 2015;124:507-14.